Accepted Manuscript

3-Amino-thieno[2,3-*b*]pyridines as microtubule-destabilising agents: Molecular modelling and biological evaluation in the sea urchin embryo and human cancer cells

Chatchakorn Eurtivong, Victor Semenov, Marina Semenova, Leonid Konyushkin, Olga Atamanenko, Jóhannes Reynisson, Alex Kiselyov

PII: S0968-0896(16)31016-1
DOI: http://dx.doi.org/10.1016/j.bmc.2016.11.041
Reference: BMC 13408

To appear in: *Bioorganic & Medicinal Chemistry*

Received Date: 18 October 2016
Revised Date: 16 November 2016
Accepted Date: 21 November 2016

Please cite this article as: Eurtivong, C., Semenov, V., Semenova, M., Konyushkin, L., Atamanenko, O., Reynisson, J., Kiselyov, A., 3-Amino-thieno[2,3-*b*]pyridines as microtubule-destabilising agents: Molecular modelling and biological evaluation in the sea urchin embryo and human cancer cells, *Bioorganic & Medicinal Chemistry* (2016), doi: http://dx.doi.org/10.1016/j.bmc.2016.11.041

3-Amino-thieno[2,3-*b*]pyridines as microtubule-destabilising agents: Molecular modelling and biological evaluation in the sea urchin embryo and human cancer cells

Chatchakorn Eurtivong[1], Victor Semenov[2], Marina Semenova[3,4], Leonid Konyushkin[2], Olga Atamanenko[2], Jóhannes Reynisson[1*], Alex Kiselyov[5]

[1] *School of Chemical Sciences, University of Auckland, New Zealand*

[2] *N. D. Zelinsky Institute of Organic Chemistry, Russian Academy of Sciences, Moscow, Russian Federation*

[3] *N. K. Kol'tsov Institute of Developmental Biology RAS, 26 Vavilov Street, 119334 Moscow, Russian Federation*

[4] *Chemical Block Ltd., 3 Kyriacou Matsi, 3723 Limassol, Cyprus*

[5] *Department of Biological and Medicinal Chemistry, Moscow Institute of Physics and Technology, Institutsky Per. 9, Dolgoprudny, Moscow Region, 141700, Russian Federation*

*To whom correspondence should be addressed: School of Chemical Sciences, University of Auckland, Private Bag 92019, Auckland 1142, New Zealand.
E-mail: j.reynisson@auckland.ac.nz, Tel. 64-9-373-7599 ext. 83746, Fax. 64-9-373-7422

Abstract

A series of 3-amino-thieno[2,3-*b*]pyridines was prepared and tested in a phenotypic sea urchin embryo assay to identify potent and specific molecules that affect tubulin dynamics. The most active compounds featured a tricyclic core ring system with a fused cycloheptyl or cyclohexyl substituent and unsubstituted or alkyl-substituted phenyl moiety tethered *via* a carboxamide. Low nano-molar potency was observed in the sea urchin embryos for the most active compounds (**1**–**5**) suggestive of a microtubule-destabilising effect. The molecular modelling studies indicated that the tubulin colchicine site is inhibited, which often leads to microtubule-destabilisation in line with the sea urchin embryo results. Finally, the identified hits displayed a robust growth inhibition (GI_{50} of 50–250 nM) of multidrug-resistant melanoma MDA-MB-435 and breast MDA-MB-468 human cancer cell lines. This work demonstrates that for the thieno[2,3-*b*]pyridines the most effective mechanism of action is microtubule-destabilisation initiated by binding to the colchicine pocket.

Keywords: Microtubule-destabilisation; sea urchin embryo assay; anticancer; thieno[2,3-*b*]pyridines; molecular modelling

Introduction

Tubulin is the main protein component of polymeric microtubules that play essential roles in mitotic spindle formation, intracellular transport, cell shape maintenance and motility.[1, 2] During mitosis, chromosomes are separated along the mitotic spindles before the formation of two daughter cells.[1, 2] It is established that deregulated division of cancer cells is dependent on mitosis making microtubules an attractive target for anticancer chemotherapeutics.[1] Drugs that affect microtubules dynamics are typically characterised as microtubule-destabilising or stabilising agents, depending on their mode of action.[3] The majority of reported microtubule-targeted drugs bind to three distinct pockets on the tubulin molecule, *i.e.*, the colchicine, *Vinca* alkaloid or taxol sites.[1, 2] Unfortunately, many anti-tubulin agents exhibit narrow efficacy/safety windows, multiple drug resistance profiles and are often generally cytotoxic to healthy cells.[3, 4] Thus, there is a considerable incentive to develop novel selective tubulin-binding agents with improved therapeutic profiles.

Recently, a series of 3-amino-thieno[2,3-*b*]pyridines (AThPs) were identified as effective anti-proliferative agents against a number of human tumour cell lines.[5-9] AThP derivatives (Figure **1**, **I**) have previously been shown to display high cytotoxicity against a tumorigenic cell line.[10] Analysis of the literature further suggests that biological target specificity for this class of compounds is dictated by the substitution pattern of the core thieno[2,3-*b*]pyridine bicyclic system. Namely, related 3-amino-2-keto-7*H*-thieno[2,3-*b*]pyridin-6-ones (Figure **1**, **II**) were found to inhibit ubiquitin C-terminal hydrolase-L1 (UCH-L1).[11] Also, the AThP core (Figure **1**, **III**) was introduced into a series of potent P-glycoprotein (P-gp), multidrug resistance-associated protein (MRP1) and the breast cancer resistance protein (BCRP1) modulators.[12] In a representative example, administration of AThP **IV** (Figure **1**) to human breast cancer cell line MDA-MB-231 caused growth restriction, rounding of cell shape, reduced motility and increase in G_2/M phase population most likely by phospholipase C-δ (PLC-δ) inhibition.[13, 14] Series of related cytotoxic molecules **V** (Figure **1**) were shown to inhibit *in vitro* tubulin polymerisation by binding to the colchicine site.[15]

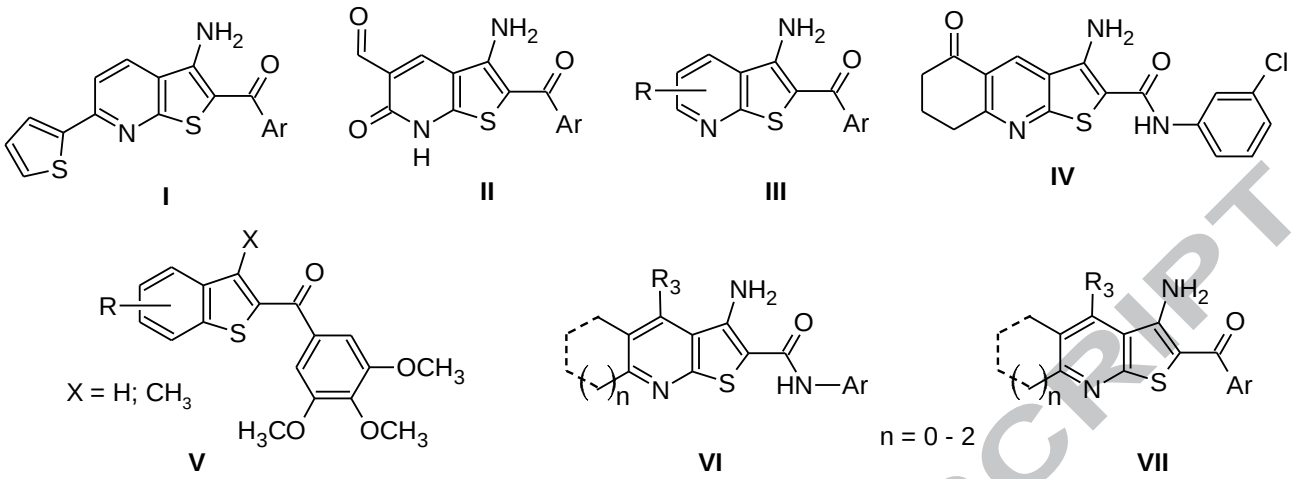

Figure 1. Biologically active 3-amino-thieno[2,3-*b*]pyridines **I**–**IV**, **VI**, **VII** and their analogs 1-benzothiophen-2-yl(3,4,5-trimethoxyphenyl)methanones **V**.

In order to glean further insight into the biological mechanism of the AThPs, series **VI** and **VII** (Figure **1**) were prepared and tested in a phenotypic sea urchin embryo assay as well as in a panel of human tumour cell lines. A set of specific developmental alterations exhibited by sea urchin embryo upon treatment with selective anti-tubulin agents has been validated and used successfully by our team in the past.[16-18] Specifically, two distinct processes during sea urchin embryogenesis are directly affected by microtubule modulators, cleavage and ciliary swimming after hatching. The compounds cause cleavage alteration/arrest with distinguishing tuberculate shape of arrested eggs and unique changes of embryo motility, namely, settlement to the bottom of the culture vessel and rapid spinning around the animal-vegetal axis. [16, 17] In this study, we used molecular modelling to elucidate the binding of the **VI** and **VII** series to tubulin, their microtubule dynamics effect in the sea urchin embryos and also the efficacy in the NCI60 human tumour cell line panel.[19]

Results and Discussion

Two distinct series of AThP **VI** (**1**–**5**) and **VII** (**6**–**40**) with carboxamide and ketone linkers, respectively, are easily accessed *via* the 3-component condensation of ketones, aldehydes and cyanothioacetamide, followed by reaction with 2-halo-acetamides or 2-halo-acetophenones as shown

in Scheme 1.[20-23] All the compounds for the biological testing were purchased from Chemical Block Ltd. (www.chemblock.com), and they were synthesised using the approach shown in Scheme 1.

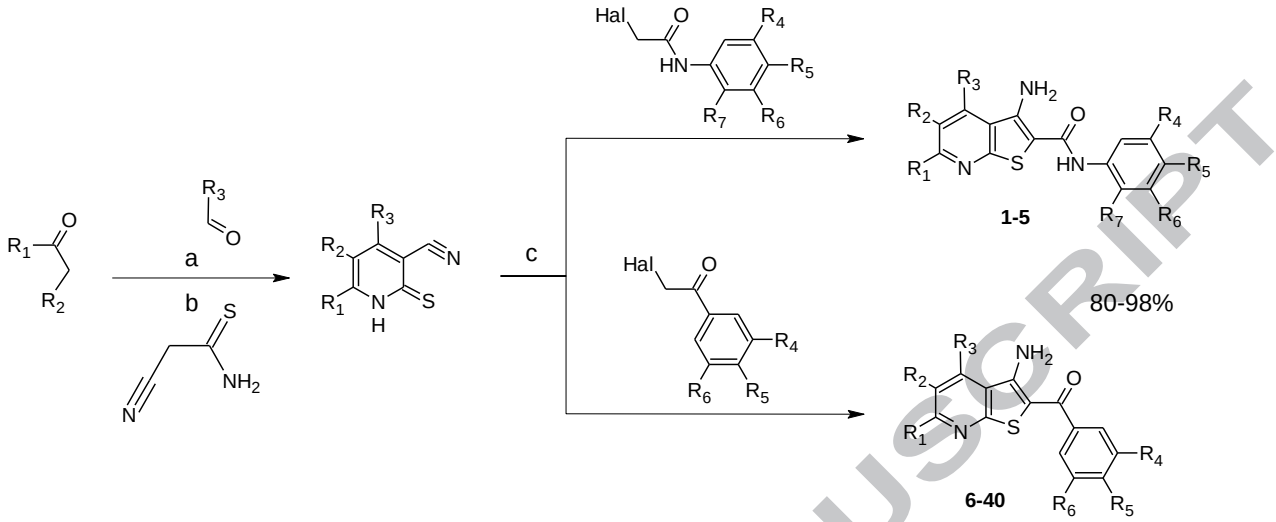

Scheme 1. Reagents and conditions: (a) R_3CHO, KOH, MeOH; (b) 2-cyanothioacetamide; (c) 2-halo-acetamides or 2-halo-acetophenones. R_1–R_7 are listed in Table 1.

Derivatives **1**–**5** have a tricyclic AThP ring system linked to a phenyl ring *via* a carboxamide moiety. Compounds **6–40** include cycloalkyl (**6–19**), bicyclic (**20**–**36**), quinuclidine (**37**–**39**), and piperidine (**40**) cores with a carbonyl linker. Specifically, molecules **20–28** contain small substitutions at position groups R_1 – R_3 in the AThP ring system, whereas molecules **29**–**36** have aromatic or heterocyclic substituents at R_1.

Prior to biological testing, the structures of the acquired compounds were confirmed by ^{1}H NMR-, MS-spectroscopies as well as melting points were determined. This data is given in the SI. AThPs **1**–**40** were tested in the phenotypic sea urchin embryo assay and in the NCI60 human tumour cell line panel and the results are given in Table **1**.

Table 1. The effects of AThPs on the sea urchin embryos and human cancer cells.

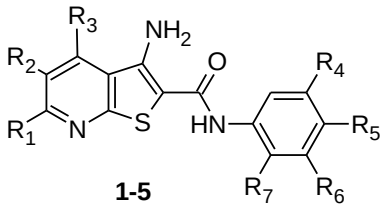

1-5

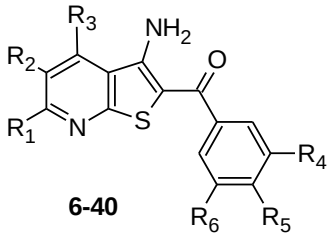

6-40

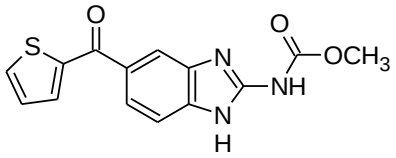

Nocodazole

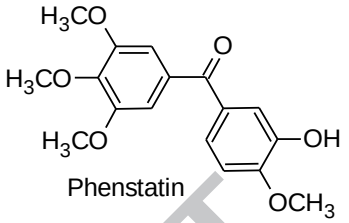

Phenstatin

Compound #	R_1	R_2	R_3	R_4	R_5	R_6	R_7	Sea urchin embryo effects, EC (μM)[a]			NCI60 screen	
								Cleavage alteration	Cleavage arrest	Embryo spinning	Mean GI, %[b]	Mean GI_{50}, μM[c]
Nocodazole	-	-	-	-	-	-	-	0.005	0.001	0.1		0.0389[d]
Phenstatin	-	-	-	-	-	-	-	0.01	0.05	0.5		0.06[e]
1	$-(CH_2)_3-$		H	H	H	Me	Me	0.05	0.5	5	76.4[f]	0.42[f]
2	$-(CH_2)_4-$		H	H	H	H	H	0.01	0.05	0.2	69.7[f]	1.00[f]
3	$-(CH_2)_4-$		H	H	H	Me	Me	0.01	0.1	0.5	ND[g]	
4	$-(CH_2)_5-$		H	H	H	H	H	0.01	0.04	0.2	85.3[f]	0.69[f]
5	$-(CH_2)_5-$		H	CF_3	H	H	H	>4	>4	>4	90.0[f]	3.09[f]
6	$-(CH_2)_3-$		H	H	Me	H	-	0.2	>4	>4	ND[g]	
7	$-(CH_2)_3-$		H	H	Br	H	-	1	>4	>4	19.3	
8	$-(CH_2)_4-$		H	H	H	H	-	0.02	0.2	0.5	ND[g]	
9	$-(CH_2)_4-$		H	H	Me	H	-	0.02	2 (TE)[h]	>4	16.4	
10	$-(CH_2)_4-$		H	H	OMe	H	-	0.5	>4	>5	ND[g]	
11	$-(CH_2)_4-$		H	H	F	H	-	0.2	>4	>4	26.7	
12	$-(CH_2)_4-$		H	H	Cl	H	-	0.5	>4	>4	7.8	
13	$-(CH_2)_4-$		H	H	Br	H	-	0.5	>4	>4	8.1	
14	$-(CH_2)_4-$		H	Me	H	Me	-	0.05	0.2 (TE)[h]	>5	78.9	0.28
15	$-(CH_2)_4-$		H	OMe	OMe	H	-	0.5	4 (TE)[h]	>5	60.5	3.24
16	$-(CH_2)_4-$		Ph	OMe	OMe	H	-	>4	>4	>4	ND[g]	
17	$-(CH_2)_4-$		4-Py	OMe	OMe	H	-	>4	>4	>4	ND[g]	
18	$-(CH_2)_4-$		H	$-OCH_2O-$		H	-	0.025	0.5 (TE)[h]	>5	ND[g]	
19	$-(CH_2)_4-$		CF_3	$-OCH_2O-$		H	-	>4	>4	>4	ND[g]	
20	H	H	H	H	Br	H	-	1	>4	>4	ND[g]	

21	Me	H	H	H	Cl	H	-	0.5	>4	>4	18.4	
22	Me	H	H	H	Me	H	-	1	4 (TE)[h]	>10	ND[g]	
23	Me	H	Me	H	Br	H	-	>4	>4	>4	ND[g]	
24	Me	H	Me	OMe	OMe	H	-	>4	>4	>4	14.2	
25	Me	H	Me	$-OCH_2CH_2O-$		H	-	1	>4	>4	2.0	
26	NH_2	CN	H	H	F	H	-	4	>4	>4	ND[g]	
27	NH_2	CN	H	H	Cl	H	-	>4	>4	>4	0.5	
28	NH_2	CN	H	OMe	OMe	H	-	4	>4	>4	4.6	
29	2-MeO-C_6H_4	H	H	OMe	OMe	H	-	NA[i]			43.5	7.94
30	2-MeO-C_6H_4	H	H	$-OCH_2O-$		H	-	>4	>4	>4	37.4	5.13
31	4-Py	H	H	OMe	OMe	H	-	4	>4	>4	17.1	
32	4-Py	H	H	$-OCH_2O-$		H	-	>4	>4	>4	ND[g]	
33	2-Thienyl	H	H	H	OMe	H	-	>4	>4	>4	ND[g]	
34	2-Thienyl	H	H	H	Cl	H	-	>4	>4	>4	ND[g]	
35	2-Thienyl	H	H	OMe	OMe	H	-	4	>4	>4	52.6	6.31
36	3,4-Methylene-dioxy-C_6H_3	H	CF_3	OMe	OMe	H	-	NA[i]			ND[g]	
37	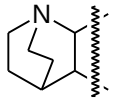		H	H	H	H	-	>4	>4	>4	7.3	
38	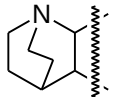		H	H	OMe	H	-	>4	>4	>4	11.5	
39	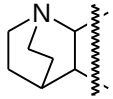		H	OMe	OMe	H	-	>4	>4	>4	11.7	
40	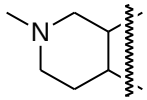		H	H	H	H	-	4	>4	>4	13.3	

[a] The sea urchin embryo assay was conducted as described previously.[16] Fertilised eggs and hatched blastulae were exposed to 2-fold decreasing concentrations of compounds. Duplicate measurements showed no differences in effective threshold concentration (EC) values.

[b] GI %: single dose inhibition of cell growth at 10 μM concentration.

[c] GI_{50}: concentration required for 50% cell growth inhibition. This is the mean for the 60 cell lines tested in the NCI60 panel.

[d] NCI ID 238159.

[e] Data from Ref.[24]
[f] Data from Ref. [6]
[g] ND: not determined.
[h] TE: tuberculate eggs typical for microtubule destabilisers.
[i] NA: not tested, insoluble in 96% ethanol.

Biological evaluation

Sea urchin embryo assay results

Analysis of the data presented in Table 1 suggests that many of the AThPs display anti-proliferative cytotoxic properties. In the *in vivo* phenotypic sea urchin embryo assay, the AThPs **1**–**4** demonstrated the strongest effect, *i.e.*, caused pronounced cleavage alteration in the 10 – 50 nM range, cleavage arrest was observed at 40 – 500 nM concentrations, and embryo spinning (0.2 – 5 μM), suggesting antimitotic microtubule-destabilising activity comparable with the activity of phenstatin, a known destabilising agent. In this series, both cycloheptane and cyclohexane rings were well tolerated, since compounds **2** and **4** exhibited similar potencies. Introduction of methyl groups at the R_6 and R_7 positions resulted in derivative **3** with similar activity, whereas the replacement of the cyclohexane ring in **3** with cyclopentane (**1**) reduced antimitotic effect. Interestingly, derivative **5** substituted with the *m*-CF_3 group at R_4 did not affect sea urchin embryo development up to 4 μM concentration.

Tricyclic AThPs **6**–**40** with carbonyl linker displayed weaker antimitotic effects upon linker replacement (ketone *vs.* amide) compared to the **1**-**4** series. For the **6**-**40** family the unsubstituted compound **8** showed the strongest microtubule-destabilising effect (embryo spinning EC = 0.5 μM). In addition, compounds **9**, **14**, **15**, and **18** can be considered as tubulin-targeting antimitotics, since they induced formation of tuberculate eggs typical for microtubule-destabilising agents.[16] The *p*-substituted methyl (**6**), methoxy (**10**), and halogen (**7**, **11**–**13**) derivatives were less active, unable to induce cleavage arrest and embryo spinning up to 4 μM concentration. Similar to series **1**–**5**, the replacement of the cyclohexane ring in **9** with cyclopentane yielded less active molecule **6**. Introduction of phenyl, 4-pyridine, and CF_3 groups at R_3 resulted in the loss of effect (**15** *vs.* **16** and **17**; **18** *vs.* **19**).

In general, bicyclic AThPs **20**–**36** as well as quinuclidine (**37**–**39**), and piperidine (**40**) derivatives exhibited minimal or no antimitotic effect. Only *p*-methyl substituted compound **22** showed weak microtubule-destabilising activity, inducing the formation of tuberculate

arrested eggs. Furthermore, AThPs **21**, **25**, **26**, **28**, **31**, and **35** displayed weak antiproliferative activity.

The sea urchin embryo tests revealed that AThPs could target not only tubulin/microtubules, but also produce other tubulin-unrelated effects. Namely, compounds **16**, **17**, **19**, **27**, **30**, **32**, and **38**–**40** were unable to alter cleavage, however caused developmental retardation and alteration at later stages of development. Interestingly, thienyl derivatives **33**–**35** exhibited specific embryotoxicity, inducing embryo disintegration and death at early pluteus, independently of the stage of exposure and treatment duration. These are qualitative observations and the mechanisms of these effects remain unclear and need further investigation in order to be established.

Cytotoxicity in human cancer cell lines

In NCI60 screen compounds **1**, **2**, **4**, and **5** at 10 μM concentration inhibited cancer cell growth by ≥70% (Table **1**). Microtubule-destabilising compounds **14** and **15** also demonstrated pronounced cytotoxicity (GI_{50} = 0.28 and 3.24 μM, respectively), whereas *p*-substituted derivatives **7**, **9**, **11**–**13** showed weaker cell growth inhibition as previously reported.[5] Bicyclic AThPs **20**–**36** (ex., **25**) exhibited minimal microtubule modulation *in vivo* along with barely detectable cytotoxic properties. Independent studies of **8** using *in vitro* (bovine) tubulin polymerisation inhibition assay[25] yielded an IC_{50} value of 13.28 μM, however the molecule did not cause cell cycle arrest in 3T3 cells.

In general, sea urchin embryo results for **1**, **2**, **4** and **5** were in good correlation with the NCI60 data reported by Arabshahi *et al.*[6], *i.e.*, human MDA-MB-435 melanoma and MDA-MB-468 breast cancer cell lines were found to be particularly sensitive to the active series and the pertinent GI_{50} values are given in Table **2**. Increased conformational flexibility by cycloalkyl ring expansion showed apparent increase in microtubule-destabilising activity and cell growth inhibition (molecules **1** *vs.* **3** and **2** *vs.* **4**). However, compound **1** showed the

strongest effect against melanoma MDA-MB-435 cell line with GI_{50} = 52 nM (Table **2**) but a relatively modest activity in the sea urchin embryo assay compared to other analogues (*e.g.*, **2**–**4**). This effect was more pronounced for compound **5**, which displayed the strongest general cancer growth inhibition with no potency in the sea urchin assay suggesting an alternative non-tubulin mediated mechanism of action. A similar outcome was observed for compound **30** (R_1 = 2-methoxyphenyl, R_2 = 3, 4-dimethoxyphenyl), it demonstrated a robust cytotoxic effect (GI_{50} = 5.13 μM) with no activity seen in the sea urchin embryo assay. These data suggest that specific anti-tubulin effect for the AThPs series is dependent on the substitution patterns for both the core and the phenyl pharmacophore.

Table 2. Effects of AThPs **1**, **2**, **4** and **5** on MDA-MB-435 human melanoma and MDA-MB-468 breast cancer cell lines.

Compound #	Mean GI, %[a]	Mean GI_{50}, nM[b]	
		MDA-MB-435[c]	MDA-MB-468[c]
1	23.6	52	197
2	30.3	172	332
4	14.7	205	254
5	10.0	2530	394

[a] GI %: single dose inhibition of cell growth at 10 μM concentration.
[b] GI_{50}: concentration required for 50% cell growth inhibition.
[c] Data from Ref. 6.

Molecular Modelling

To gain further insight into mode of binding, the AThPs derivatives were docked to the three main binding sites of tubulin, i.e., colchicine, *Vinca* alkaloid and taxol pockets using the respective Protein Data Bank (PDB)[26, 27] structures (IDs: 4O2B,[28] 4EB6[29] and 1JFF[30]). Four scoring functions were employed: GoldScore (GS),[31] ChemScore (CS),[32, 33] ChemPLP[34] and ASP.[35] The co-crystallised ligands were removed and re-docked to their respective binding sites. Excellent root-mean-square deviations (RMSD) only including the heavy atoms for Colchicine was obtained with average of 0.394 Å for the four scoring functions used,

Paclitaxel also gave good results with an average of 1.625 Å but only GS reproduced the experimentally derived configuration of Vinblastine adequately at 1.307 Å (see supplementary Table **S1**), with the GS algorithm giving the most consistent results in general. The results of the binding scores (see Table **S2** in the **SI**) against the three possible binding pockets indicate that the Colchicine site is favoured when the GS scores are considered, it has +60 whereas the Vinblastine and Paclitaxel pockets only have +50 arbitrary units. When the scores for the Colchicine and Paclitaxel sites are compared ChemPLP gives considerably better perditions for the former but ASP and CS give similar results. ChemPLP has been reported to be the best performing scoring function available in the GOLD package.[36] This is supported by experimental results, AThPs do not have the same mode of action as Paclitaxel, *i.e.*, no mitotic microtubule bundles were seen for the MDA-MB-231 breast cancer cells upon administration of an AThPs analogue as expected for a compound sharing a mode of action with Paclitaxel.[14] Thus, the docking results indicate that the Colchicine site is favoured as suggested by Romangoli *et al*.[15] Occupation of this site often causes destabilistation of microtubules, which is in line with the sea urchin results. Admittedly, it would had been better to have better predictions for the Vinblastine binding pocket.

Modelling studies for compounds **1**-**5** for the Colchicine pocket predicted hydrogen bonding with the amino acid residues Val181 and Thr179 and hydrophobic contacts between the phenyl ring and lipophilic regions inside the β–subunit cavity where side chains of hydrophobic amino acid residues of Ala316, Leu255 Val181 form a cavity. The cycloakyl moiety is predicted to be oriented towards a large hydrophobic area within the α/β interface facilitating lipophilic contacts with the amino acid residues Leu248, Tyr224, Gly143, and Ala180 as shown in Fig. **2B** and **2D**. Weak anti-tubulin activities of **6**–**46** tricyclic, bicyclic and quinuclidinyl AThPs can be explained by limited interaction with the

α/β tubulin interface. This hypothesis is supported by the observation that an increase in cycloalkyl ring size correlates with enhanced tubulin-destabilising effects of the AThPs.

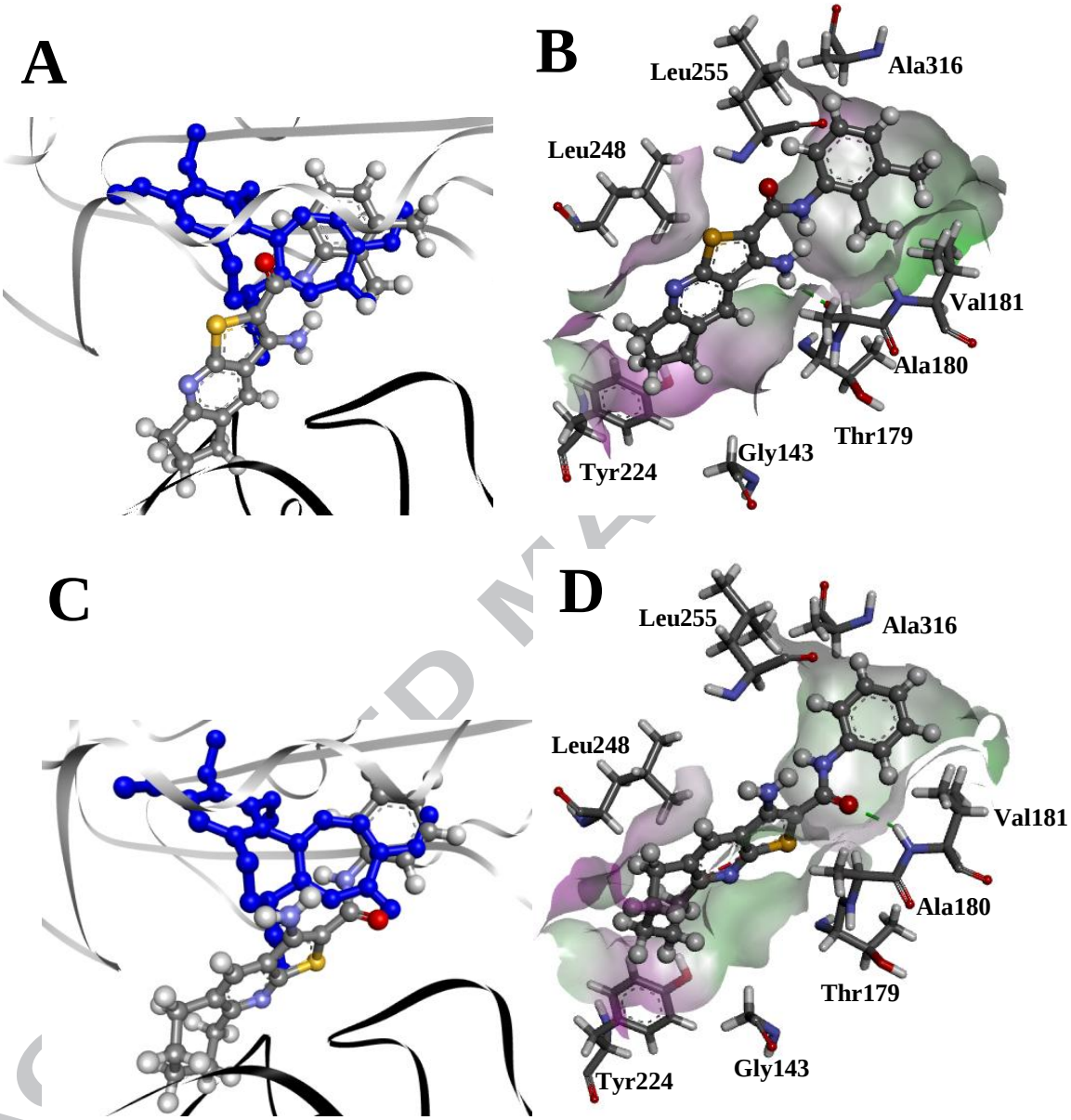

Figure 2. Binding poses of compounds **1** (**A** and **B**) and **4** (**C** and **D**). Colchicine (blue) is overlain with the ligands (**A** and **C**). The grey and black polypeptide ribbons belong to the β- and α-chains, respectively. Green dotted lines represent hydrogen bonds. The binding site of the protein is rendered where grey is neutral and green and pink represent hydrogen bond acceptor and donor groups (**B** and **D**).

The calculated molecular descriptors (MW, log P, HD, HA, PSA and RB) for derivatives **1-40** are all within the boundaries of *drug – like* chemical space with two minor exceptions, derivative **16** has a log P value of 5.3 and the MW of derivative **36** is 502.5 g mol^{-1}. Indeed,

many of the derived values lie within *lead-like* chemical space (for definition of these regions see ref.[37], references therein). The calculated values are given in Table S3 in the Supplementary Information section.

Conclusion

In this work it is shown that tubulin destabilisation is one of the main biological mechanism of action for the AThPs based on the sea urchin embryo data. Derivatives **1**–**4** have a low nano-molar activity but the rest of the compounds are less active. An amide linker between the thienopyridine core and the phenyl group is crucial for the activity, which can be rationalised with enhanced lipophilic contact at the α/β interface in tubulin compared to the analogues containing a ketone linker according to molecular modelling to the colchicine site. The potency in the sea urchin assay is reflected for the NCI60 human tumour panel with some notable exceptions (*e.g.*, derivative **5**) that suggested that this class of compounds has a number of modes of action, which can be modulated with, *e.g.*, different substitution pattern on the phenyl ring. It is clear that more work is required in order to identify all of the biological targets of the AThPs but the results presented here substantially advances our insight into their mechanism of action.

Methodology

Analysis of AThPs derivatives

^{1}H NMR spectra were recorded on a Bruker DRX-500 (500.13 MHz) instrument. Chemical shifts were stated in parts per million (ppm) and referenced to the appropriate NMR solvent peak(s). Low resolution mass spectra (*m*/*z*) were recorded on a Finnigan MAT/INCOS 50 mass spectrometer at 70 eV using direct probe injection. Melting points were measured on a Boetius melting point apparatus and were uncorrected.

Phenotypic sea urchin embryo assay

Adult sea urchins, *Paracentrotus lividus* L. (Echinidae), were collected from the Mediterranean Sea on the Cyprus coast and kept in an aerated seawater tank. Gametes were obtained by intracoelomic injection of 0.5 M KCl. Eggs were washed with filtered seawater and fertilised by adding drops of diluted sperm. Embryos were cultured at room temperature under gentle agitation with a motor-driven plastic paddle (60 rpm) in filtered seawater. The embryos were observed with a Biolam light microscope (LOMO, St. Petersburg, Russia). For treatment with the test compounds, 5 mL aliquots of embryo suspension were transferred to six-well plates and incubated as a monolayer at a concentration up to 2000 embryos/mL. Stock solutions of compounds were prepared in DMSO at 10 mM concentration followed by a 10-fold dilution with 96% EtOH. This procedure enhanced the solubility of the test compounds in the salt-containing medium (seawater), as evidenced by microscopic examination of the samples. The maximal tolerated concentrations of DMSO and EtOH in the *in vivo* assay were determined to be 0.05% and 1%, respectively. Higher concentrations of either DMSO (≥0.1%) or EtOH (>1%) caused nonspecific alteration and retardation of the sea urchin embryo development independent of the treatment stage. Nocodazole (Sigma-Aldrich) and phenstatin (synthesised as reported previously[38]) served as reference compounds. The antiproliferative activity was assessed by exposing fertilised eggs (8–20 min after fertilisation, 45–55 min before the first mitotic cycle completion) to 2-fold decreasing concentrations of the compound. Cleavage alteration and arrest were clearly detected at 2.5–5.5 h after fertilisation. The effects were estimated quantitatively as an effective threshold concentration, resulting in cleavage alteration and embryo death before hatching or full mitotic arrest. At these concentrations all tested microtubule destabilisers caused 100% cleavage alteration and embryo death before hatching, whereas at 2-fold lower concentrations the compounds failed to produce any effect. For microtubule-destabilising activity, the

compounds were tested on free-swimming blastulae just after hatching (8–10 h after fertilisation), which originated from the same embryo culture. Embryo spinning was observed after 15 min to 20 h of treatment, depending on the structure and concentration of the compound. Both spinning and lack of forward movement were interpreted to be the result of the microtubule-destabilising activity of a molecule. Video illustrations are available at http://www.chemblock.com. Experiments with the sea urchin embryos fulfil the requirements of biological ethics. The artificial spawning did not result in animal death, embryos develop outside the female organism, and both post-spawned adult sea urchins and the excess of intact embryos are returned to the sea, their natural habitat.

NCI60 assay

Compounds **7**, **9**, **11-15**, **21**, **24**, **25**, **27-29**, **31**, **35**, **37-40** were submitted to the National Cancer Institute's Developmental Therapeutic Program (DTP) where they were screened against a panel of sixty human tumour cell lines first at 10 μM and for active ligands dose response curves were generated (NCI60, for further information see ref.[19, 39-40] and references therein). Furthermore, the full description of the protocol is given in the Supplementary Information.

Molecular modelling

The compounds were docked to the crystal structures of tubulin with the respective PDB IDs: 4O2B (resolution 2.3 Å)[28], 4EB6 (resolution 3.47 Å)[29] and 1JFF (resolution 3.5 Å).[30] The Scigress v2.6[41] was used to prepare the crystal structure for docking, *i.e.* hydrogen atoms were added, the co-crystallised ligands were removed as well as crystallographic water molecules. The Scigress software suite was also used to build the chemical structures and were optimised using the MM2[42] force field. The centre of the binding were defined in crystal

structures: 4O2B as C3 on Colchicine (x = 13.222, y = 8.371, z = -23.331), 4EB6 as C58 on Vinblastine (x = 13.391, y = 90.610, z = 103.739) and 1JFF as O11 on Paclitaxel (x = 1.403, y = -16.979, z = 16.391) with 10 Å radius. Fifty docking runs were allowed for each ligand with default search efficiency (100%). The basic amino acids lysine and arginine were defined as protonated. Furthermore, aspartic and glutamic acids were assumed to be deprotonated. The GoldScore (GS),[31] ChemScore (CS),[32, 33] ChemPLP[34] and ASP[35] scoring functions were implemented to validate the predicted binding modes and relative energies of the ligands using the GOLD v5.4.0 software suite.

The QikProp 3.2[43] software package was used to calculate the molecular descriptors of the compounds. The reliability of the prediction power of QikProp is established for the molecular descriptors used in this study.[44]

References

1. Jordan, M. A.; Wilson, L. *Nat. Rev. Cancer* **2004,** *4*, 253-265.
2. Stanton, R. A.; Gernert, K. M.; Nettles, J. H.; Aneja, R. *Med. Res. Rev.* **2011,** *31*, 443-481.
3. van Vuuren, R. J.; Visagie, M. H.; Theron, A. E.; Joubert, A. M. *Cancer Chemother. Pharmacol.* **2015,** *76*, 1101-1112.
4. Ecsedy, J. A.; Manfredi, M.; Chakravarty, A.; D'Amore, N., Current and Next Generation Antimitotic Therapies in Cancer. In *Signaling Pathways in Cancer Pathogenesis and Therapy*, Frank, A. D., Ed. Springer New York: New York, NY, 2012; pp 5-21.
5. Arabshahi, H. J.; Leung, E.; Barker, D.; Reynisson, J. *Med. Chem. Comm.* **2014,** *5*, 186-191.
6. Arabshahi, H. J.; van Rensburg, M.; Pilkington, L. I.; Jeon, C. Y.; Song, M.; Gridel, L.-M.; Leung, E.; Barker, D.; Vuica-Ross, M.; Volcho, K. P.; Zakharenko, A. L.; Lavrik, O. I.; Reynisson, J. *Med.Chem.Comm.* **2015,** *6*, 1987-1997.
7. Eurtivong, C.; Reynisdóttir, I.; Kuczma, S.; Furkert, D. P.; Brimble, M. A.; *Biorg. Med. Chem.* **2016**, *24*, 3521-3526.
8. Feng, L.; Reynisdóttir, I.; Reynisson, J. *Eur. J. Med. Chem.* **2012,** *54*, 463-469.
9. Hung, J. M.; Arabshahi, H. J.; Leung, E.; Reynisson, J.; Barker, D. *Eur. J. Med. Chem.* **2014,** *86*, 420-437.
10. Hayakawa, I.; Shioya, R.; Agatsuma, T.; Furukawa, H.; Sugano, Y. *Bioorg. Med. Chem. Lett.* **2004,** *14*, 3411–3414.

11. Mermerian, A. H.; Case, A.; Stein, R. L.; Cuny, G. D. *Bioorg. Med. Chem. Lett.* **2007,** *17*, 3729–3732.
12. Krauze, A.; Grinberga, S.; Krasnova, L.; Adlere, I.; Sokolova, E.; Domracheva, I.; Shestakova, I.; Andzans, Z.; Duburs, G. *Bioorg. Med. Chem.* **2014,** *22*, 5860-5870.
13. Leung, E.; Hung, J. M.; Barker, D.; Reynisson, J. *Med. Chem. Comm.* **2014,** *5*, 99-106.
14. Reynisson, J.; Jaiswal, J. K.; Barker, D.; D'Mello S, A.; Denny, W. A.; Baguley, B. C.; Leung, E. Y. *Cancer Cell Int.* **2016,** *16*, 18.
15. Romagnoli, R.; Baraldi, P. G.; Kimatrai Salvador, M.; Preti, D.; Aghazadeh Tabrizi, M.; Bassetto, M.; Brancale, A.; Hamel, E.; Castagliuolo, I.; Bortolozzi, R.; Basso, G.; Viola, G. *J. Med. Chem.* **2013,** *56*, 2606-18.
16. Semenova, M. N.; Kiselyov, A.; Semenov, V. V. *Biotechniques* **2006,** *40*, 765-774.
17. Nishioka, D.; Marcell, V.; Cunningham, M.; Khan, M.; Von Hoff, D. D.; Izbicka, E., The Use of Early Sea Urchin Embryos in Anticancer Drug Testing. In *Novel Anticancer Drug Protocols*, Buolamwini, J. K.; Adjei, A. A., Eds. Humana Press: Totowa, NJ, 2003; pp 265-276.
18. Kiselyov, A. S.; Semenova, M. N.; Chernyshova, N. B.; Leitao, A.; Samet, A. V.; Kislyi, K. A.; Raihstat, M. M.; Oprea, T.; Lemcke, H.; Lantow, M.; Weiss, D. G.; Ikizalp, N. N.; Kuznetsov, S. A.; Semenov, V. V. *Eur. J. Med. Chem.* **2010,** *45*, 1683-1697.
19. Shoemaker, R. H. *Nat. Rev. Cancer* **2006,** *6*, 813-823.
20. Lockman, J. W.; Reeder, M. D.; Suzuki, K.; Ostanin, K.; Hoff, R.; Bhoite, L.; Austin, H.; Baichwal, V.; J.A., W. *Bioorg. Med. Chem. Lett.* **2010,** *20*, 2283–2286.
21. El-Dean, A. M. K.; Shaker, R.; El-Hassan, A. A. A.; Abdel Latif, F. F. A. *J. Chin. Chem. Soc.* **2004,** *51*, 335-345.
22. Nesterov, V. N.; Rodinovskaya, L. A.; Litvinov, V. P.; Sharanin, Y. A.; Shestopalov, A. M.; Mortikov, V. Y.; Shvedov, V. I.; Shklover, V. E.; Struchkov, Y. T. *Russ. Chem. Bull.* **1988,** *37*, 129-134.
23. Kislyi, V. P.; Nikishin, K. G.; Kruglova, E. Y.; Shestopalov, A. M.; Semenov, V. V.; Gakh, A. A.; Buchanan III, A. C. *Tetrahedron* **1996,** *52*, 10841–10848.
24. Pettit, G. R.; Toki, B.; Herald, D. L.; Verdier-Pinard, P. V.; Boyd, M. R.; Hamel, E.; Pettit, R. K. *J. Med. Chem.* **1998,** *41*, 1688–1695.
25. Ouyang, X.; Chen, X.; Piatnitski, E. L.; Kiselyov, A. S.; He, H.; Mao, Y.; Pattaropong, V.; Yu, Y.; Kim, K. H.; Kincaid, J.; Smith II, L.; Wong, W. C.; Lee, S. P.; Milligan, D. L.; Malikzay, A.; Fleming, J.; Gerlak, J.; Deevi, D.; Doody, J. F.; Chiang, H.; Patel, S. N.; Wang, Y.; Rolser, R. L.; Kussie, P.; Labelle, M.; Tuma, M. C. *Bioorg. Med. Chem. Lett.* **2005,** *15*, 5154–5159.
26. Berman, H.; Henrick, K.; Nakamura, H. *Nat. Struct. Biol.* **2003,** *10*, 980.
27. Berman, H. M.; Westbrook, J.; Feng, Z.; Gilliland, G.; Bhat, T. N.; Weissig, H.; Shindyalov, I. N.; Bourne, P. E. *Nuc.Acids Res.* **2000,** *28*, 235-242.
28. Prota, A. E.; Danel, F.; Bachmann, F.; Bargsten, K.; Buey, R. M.; Pohlmann, J.; Reinelt, S.; Lane, H.; Steinmetz, M. O. *J. Mol. Biol.* **2014,** *426*, 1848-1860.
29. Ranaivoson, F. M.; Gigant, B.; Berritt, S.; Joullie, M.; Knossow, M. *Acta Crystallographica Section D* **2012,** *68*, 927-934.
30. Löwe, J.; Li, H.; Downing, K. H.; Nogales, E. *J. Mol. Biol.* **2001,** *313*, 1045-1057.
31. Jones, G.; Willet, P.; Glen, R. C.; Leach, A. R.; Taylor, R. *J.Mol.Biol.* **1997,** *267*, 727-748.
32. Eldridge, M. D.; Murray, C.; Auton, T. R.; Paolini, G. V.; Mee, P. M. *J. Comp. Aid. Mol. Design* **1997,** *11*, 425-445.

33. Verdonk, M. L.; Cole, J. C.; Hartshorn, M. J.; Murray, C. W.; Taylor, R. D. *Proteins* **2003,** *52*, 609-623.
34. Korb, O.; Stützle, T.; Exner, T. E. *J. Chem. Inf. Model.* **2009,** *49*, 84-96.
35. Verdonk, M. L.; Chessari, G.; Cole, J. C.; Hartshorn, M.; Murray, C. W.; Nissink, J. W. M.; Taylor, R. D.; Taylor, R. *J. Med. Chem.* **2005,** *48*, 6504-6515.
36. Liebeschuetz, J. W.; Cole, J. C.; Korb, O. *J. Comput. Aided Mol. Des.* **2012,** *26*, 737–748.
37. Zhu, F.; Logan, G.; Reynisson, J. *Mol. Inf.* **2012,** *31*, 847 – 855.
38. Titov, I. Y.; Sagamanova, I. K.; Gritsenko, R. T.; Karmanova, I. B.; Atamanenko, O. P.; Semenova, M. N.; Semenov, V. V. *Bioorg. Med. Chem. Lett.* **2011,** *21*, 1578–1581.
39. Alley, M. C.; Scudiero, D. A.; Monks, P. A.; Hursey, M. L.; Czerwinski, M. J.; Fine, D. L.; Abbott, B. J.; Mayo, J. G.; Shoemaker, R. H.; Boyd, M. R. *Cancer Res.* **1988,** *48*, 589-601.
40. Boyd, M. R.; Paull, K. D. *Drug Dev. Res.* **1995,** *34*, 91-109.
41. *Scigress v2.6*, Fijitsu Limited: 2008 - 2016.
42. Allinger, N. L. *J. Am. Chem. Soc.* **1977,** *99*, 8127-8134.
43. *QikProp*, v3.2; Schrödinger: New York, 2009.
44. Ioakimidis, L.; Thoukydidis, L.; Naeem, S.; Mirza, A.; Reynisson, J. *QSAR Comb. Sci.* **2008,** *27*, 445-456.

Graphical abstract

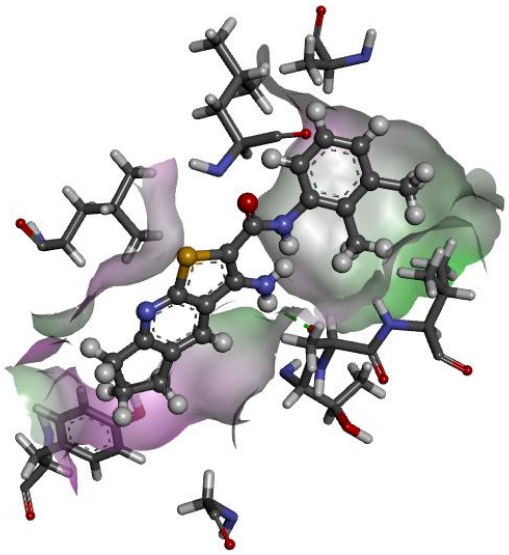

The thieno[2,3-*b*]pyridines are shown to induce microtubule-destabilisation explaining their efficacy against cancer cells.